Ibn Al Haitham Journal for Pure and Applied Science

Journal homepage: http://jih.uobaghdad.edu.iq/index.php/j/index

Hall and Joule's heating Influences on Peristaltic Transport of Bingham plastic Fluid with Variable Viscosity in an Inclined Tapered Asymmetric Channel

Rasha Yousif Hassen **Hayat A. Ali**

Department of Mathematics and Application of Computer, University of Technology,

rashamath80@yahoo.com 100048@uotechnology.edu.iq

Article history: Received 20, January, 2020, Accepted 26, February, 2020, Published in January 2021

Doi: 10.30526/34.1.2554

Abstract

This paper presents an investigation of peristaltic flow of Bingham plastic fluid in an inclined tapered asymmetric channel with variable viscosity. Taking into consideration Hall current, velocity, thermal slip conditions, Energy equation is modeled by taking Joule heating effect into consideration and by holding assumption of long wavelength and low Reynolds number approximation, these equations are simplified into a couple of non-linear ordinary differential equations that are solved by using perturbation technique. Graphical analysis has been involved for various flow parameters emerging in the problem. We observed two opposite behaviors for Hall parameter and Hartman number on velocity axial and temperature curves.

Keywords: Heat Transfer, Hall Effect, Joule's Heating, Bingham plastic Fluid, Tapered Channel.

1. Introduction

Peristaltic transport is a successive sinusoidal waves movement of fluids along a flexible channel walls. It is naturally found in human living body such as urine movement from kidney to bladder, food swallowing process and blood flow in the small vessels [1- 3]. Moreover, the peristaltic transport of non- Newtonian fluid gained much attention in various modern industrial and biomedical phenomena like polymer industry and artificial hearts that their devices designed in a manner where the fluid flows without internal moving parts [4-6]. Inspired by this fact and since the modern industrial fluids are characterized by their variable viscosity, a few researchers indicate studies regarding the peristaltic transport of fluids having variable viscosity. Adnan and Abdulhadi [7] analyzed the effect of an inclined magnetic field on peristaltic flow of Bingham plastic fluid in an inclined symmetric channel with slip conditions. In the same year Adnan and Abdulhadi [8] investigated the peristaltic flow of the

Bingham plastic fluid in a curved channel. Hayat et al. [9] studied the effect of soret and dufour on the peristaltic transport of Bingham plastic fluid considering magnetic field. While Lakshminarayana et al. [10] investigated the heat transfer and the effect of slip condition and wall properties on the peristaltic transport of Bingham fluid. Ara et al. [11] explored the Jeffery- Hamel flow of Bingham plastic fluid in converging channel in the presence of external magnetic field. However, Salih [12] illustrated the influence of varying temperature and concentration on (MHD) peristaltic transport of Jeffery fluid with variable viscosity through porous channel. For more information see [7,13].

In this paper, the influence of Hall and Joule's heating on the peristaltic flow of Bingham plastic fluid passing through an inclined tapered asymmetric channel with variable viscosity is studied. A long wave number and low Reynolds number are taken into consideration to simplify the problem. Perturbation technique is used to solve and find the last shape of stream function.

Finally, the effects of various parameters on axial velocity, temperature, stream function and heat transfer coefficients are discussed graphically.

2. Mathematical Modeling

The peristaltic transport of an incompressible Bingham plastic fluid in a tapered inclined channel at an angle α which is an asymmetric channel with a total width$(2d)$ is considered. Characterizing the flow by the existence of a strong transverse magnetic field $B = (0, 0, \beta_0)$. A magnetic Reynolds number is taken small and the induced magnetic field is prescribed neglected. The flow is achieved by the peristaltic waves of length λ with different amplitude and phases moving with a constant speed c along the channels walls.

The geometry of the walls surfaces is described by

$$Y_1 = H_1(\bar{X}, t) = d + m_1\bar{X} + a_1 Cos\left(\frac{2\pi(\bar{X}-ct)}{\lambda}\right) \quad (1)$$

$$Y_2 = H_2(\bar{X}, t) = -d - m_1\bar{X} - a_2 Cos\,(2\pi(\bar{X} - ct)/\lambda + \emptyset) \quad (2)$$

Where Y_1, Y_2 are the upper and lower wall respectively, m_1 is the non-uniform parameter, a_1, a_2 are the wave amplitudes, t is the time and $(\bar{X}, \bar{Y})$ the rectangular coordinates in a fixed frame. $\emptyset$ Is the phase different and $\emptyset \in [0, \pi]$ such that when $\emptyset = 0$ corresponds to asymmetric channel with waves out of phase, and when $\emptyset = \pi$, the waves are in phase. Further $a, b, d\ and\ \emptyset$ satisfy the necessary condition

$$a^2 + b^2 + 2abd\ cos\emptyset \leq (2d)^2 \quad (3)$$

By applying the generalized Ohm's law [2], we include the Hall current as follows

$$\vec{F} = \vec{J} \times \vec{B} \quad (4)$$

Such that

$$\vec{J} = \sigma[\vec{V} \times \vec{B} - \frac{1}{en}\left(\vec{J} \times \vec{B}\right)] \quad (5)$$

Hence,

$$\vec{F} = \left(\frac{-\sigma {\beta_0}^2 (U - mV)}{1+m^2}, \frac{\sigma {\beta_0}^2 (V + mU)}{1+m^2}, 0\right) \quad (6)$$

In which $\vec{F}$ is the magnetic force, $\vec{J}$ assigns to the current density vector, $\vec{V} = (U, V, 0)$ the velocity field, σ the electrical conductivity, n the number density of electron, e the electric charge, β_0 the magnetic field strength and $\left(m = \frac{\sigma \beta_0}{en}\right)$ the Hall parameter.

The fluid satisfies Bingham plastic model and its extra stress tensor is given as follows [11]:

$$\left.\begin{aligned} \bar{S} &= \left(\mu(\bar{Y}) + \frac{\tau_y}{\gamma\cdot}\right)\bar{A}_1 \quad \text{For} \quad \tau \geq \tau_y \\ \bar{S} &= 0 \quad \text{For} \quad \tau < \tau_y \end{aligned}\right\} \quad (7)$$

Such that

$$\bar{A}_1 = \nabla\vec{V} + \left(\nabla\vec{V}\right)^T \quad (8)$$

And

$$\gamma\cdot = \sqrt{\frac{trac(\bar{A}_1)^2}{2}} \quad (9)$$

$\bar{S}$ represents the extra stress tensor,$\nabla = (\partial/\partial\bar{X}, \partial/\partial\bar{Y}, 0)$ the gradient vector, τ_y the yield stress $\bar{A}_1$is the first Rivlin- Erickson, and $\mu(\bar{Y})$ is the dynamic variable viscosity.

The fundamental equations of the flow can be written as below:

$$div\,\bar{V} = 0 \quad (10)$$

X-component of momentum equation

$$\rho\left(\frac{d\bar{U}}{dt} + \bar{U}\frac{\partial\bar{U}}{\partial\bar{X}} + \bar{V}\frac{\partial\bar{U}}{\partial\bar{Y}}\right) = -\frac{\partial\bar{P}}{\partial\bar{X}} + \frac{\partial\bar{S}_{\bar{X}\bar{X}}}{\partial\bar{X}} + \frac{\partial\bar{S}_{\bar{X}\bar{Y}}}{\partial\bar{Y}} - \frac{\sigma\beta^2(\bar{U} - m\,\bar{V})}{1+m^2} + \rho g\,\mathrm{Sin}\,\alpha - \frac{\mu}{\kappa}\bar{U} \quad (11)$$

Y-component of momentum equation

$$\rho\left(\frac{d\bar{V}}{dt} + \bar{U}\frac{\partial\bar{V}}{\partial\bar{X}} + \bar{V}\frac{\partial\bar{V}}{\partial\bar{Y}}\right) = -\frac{\partial\bar{P}}{\partial\bar{Y}} + \frac{\partial\bar{S}_{\bar{X}\bar{Y}}}{\partial\bar{X}} + \frac{\partial\bar{S}_{\bar{Y}\bar{Y}}}{\partial\bar{Y}} - \frac{\sigma\beta^2(\bar{V} + m\,\bar{U})}{1+m^2} + \rho g\,\mathrm{Cos}\,\alpha - \frac{\mu}{\kappa}\bar{V} \quad (12)$$

And

Energy equation with Joule heating effect is

$$\rho c_P\left(\frac{\partial T}{\partial\bar{t}} + \bar{U}\frac{\partial T}{\partial\bar{X}} + \bar{V}\frac{\partial T}{\partial\bar{Y}}\right) = K\left(\frac{\partial^2 T}{\partial\bar{X}^2} + \frac{\partial^2 T}{\partial\bar{Y}^2}\right) + (\bar{S}_{\bar{Y}\bar{Y}} - \bar{S}_{\bar{X}\bar{X}})\frac{\partial\bar{V}}{\partial\bar{Y}} + \bar{S}_{\bar{X}\bar{Y}}\left(\frac{\partial\bar{U}}{\partial\bar{Y}} + \frac{\partial\bar{V}}{\partial\bar{X}}\right) + \frac{\sigma {\beta_0}^2(\bar{U}^2 + \bar{V}^2)}{1+m^2} \quad (13)$$

In which $\sigma, K, \kappa, \bar{P}, \mu, \rho, c_P, g$ are the electrical conductivity, the thermal conductivity, the porosity parameter, the dynamic viscosity, the density, the specific heat, and the gravity respectively.

The corresponding boundary slip conditions are

$$\left.\begin{aligned} \bar{U} \mp \gamma \bar{S}_{xy} = 0 \;\; at \;\;\; \bar{Y} = H_1, H_2 \\ T \mp \beta_1 \frac{\partial T}{\partial y} = T_0 \;\; at \;\;\; \bar{Y} = H_1, H_2 \end{aligned}\right\} \tag{14}$$

And the wall flexibility condition is

$$\left[-\tau \frac{\partial^3}{\partial \bar{X}^3} + m_2 \frac{\partial^3}{\partial \bar{X} \partial t^2} + d' \frac{\partial^2}{\partial t \partial \bar{X}}\right] \bar{Y} = \frac{\partial \bar{P}}{\partial \bar{X}} \qquad at \;\;\; \bar{Y} = H_1, H_2 \tag{15}$$

Where $T_0, \tau, m_2, d', \gamma, \beta_1$ are the temperature at the upper and lower walls, the elastic tension, the mass per unit area and the coefficient of viscous damping, velocity slip coefficient, and temperature slip coefficient respectively.

Dimensional analysis is used for normalizing the flow equations Eqs. (7) - (15) by using the following as bellows:

$$x = \frac{\bar{X}}{\lambda} \;, y = \frac{\bar{Y}}{d} \;, \;\; u = \frac{\bar{U}}{c} \;, v = \frac{\bar{V}}{c} \;, h_1 = \frac{H_1}{d}, h_2 = \frac{H_2}{d} \;, p = \frac{d^2 \bar{p}}{\lambda \mu c}, \delta = \frac{d}{\lambda} \;, \gamma^* = \frac{\gamma}{d} \;, \beta_1^* = \frac{\beta_1}{d}, S = \frac{d\bar{S}(\bar{X})}{\mu c} \;, Re = \frac{\rho c d}{\mu}, \;\; \theta = \frac{T - T_0}{T_0}, E_1 = \frac{-\tau d^3}{\lambda^3 \mu c} \;, E_2 = \frac{m_2 c d^3}{\lambda^3 \mu c}, E_3 = \frac{d' d^3}{\lambda^2 \mu}, Pr = \frac{\mu c_P}{k} \;, H = \beta_0 d \sqrt{\frac{\sigma}{\mu}} \;, E_c = \frac{c^2}{c_P T_0} \;, Br = E_c Pr \;, \;\; Fr = \frac{c}{\sqrt{gd}} \;, d_1 = \frac{a_1}{d} \;, d_2 = \frac{a_2}{d} \;, {m_1}^* = \frac{m_1 \lambda}{d}, Bn = \frac{d\tau_y}{\mu c}, \mu(\bar{Y}) = \frac{\mu(y)}{\mu} \tag{16}$$

Where δ is the wave number, E_1 the wall elastance parameter, E_2 the mass per unit area parameter, $E_3$the wall damping parameter, Re the Reynolds number, Pr the Prandtl number, H Hartman number, Ec Eckret number, Br Brinkman number, Fr Froude number, ${m_1}^*$ the dimensionless non-uniform parameter, h_1 the dimensionless lower wall surface, h_2 upper wall surface, x, y components of the dimensionless coordinates, u axial velocity, v transverse component of velocity, ϵ the fluid dimensionless viscosity parameter, $\gamma^{\cdot}, \beta_1^*$ the dimensionless velocity and thermal slip parameters respectively and Bn

Bingham number. Note that we omitted asterisks for simplicity

Introducing the stream function $\psi(x, y, t)$ and make use of the following relation

$$u = \psi_y, \;\; v = -\delta \psi_x$$

Applying Eq. (17) into Eqs. (9) – (16) and making use of Eq. (17), the continuity equation (11) vanishs identically, other flow equations take the following form

$$\delta Re\left(\psi_{ty} + \psi_y \psi_{xy} - \delta \psi_x \psi_{xy}\right) = -P_x + \delta \frac{\partial S_{xx}}{\partial x} + \frac{\partial S_{xy}}{\partial y} - \frac{H^2}{(1+m^2)}\left(\psi_y + \delta m \psi_x\right) - \frac{\psi_y}{\kappa} + \frac{Re}{(Fr)^2} \; sin\alpha \tag{17}$$

$$\delta^2 Re\left(-\delta^2 \psi_{tx} - \delta^2 \psi_y \psi_{xx} + \delta^3 \psi_x \psi_{xy}\right) = -P_y + \delta \frac{\partial S_{yy}}{\partial y} + \delta^2 \frac{\partial S_{yx}}{\partial x} - \frac{H^2 \delta}{(1+m^2)}\left(-\delta \psi_x + m \psi_y\right) - \frac{\psi_y}{\kappa} - \frac{\delta Re}{(Fr)^2} \; cos\alpha \tag{18}$$

$$RePr\left(\delta\frac{\partial\theta}{\partial t}+\delta\psi_y\frac{\partial\theta}{\partial x}-\delta\psi_x\frac{\partial\theta}{\partial y}\right)=$$
$$\delta^2\frac{\partial^2\theta}{\partial x^2}+\frac{\partial^2\theta}{\partial y^2}+BrS_{xy}\left(\psi_{yy}-\delta^2\psi_{xx}\right)+\frac{H^2Br}{(1+m^2)}\left((\psi_y)^2+\delta^2(\psi_x)^2\right)+\delta Br\left(S_{xx}-S_{yy}\right)\psi_{xy}\ \ldots(19)$$

Adopting the assumptions of peristaltic long wavelength and low Reynolds number, Eqs. (17)-(19) will be reduced into following form

$$P_x=\frac{\partial S_{xy}}{\partial y}-\left(\frac{H^2}{(1+m^2)}+\frac{1}{\kappa}\right)\psi_y+\frac{Re}{(Fr)^2}\,sin\alpha, \tag{20}$$

$$P_y=0, \tag{21}$$

$$\frac{\partial^2\theta}{\partial y^2}=BrS_{xy}\psi_{yy}+\frac{H^2Br}{(1+m^2)}(\psi_y)^2, \tag{22}$$

$$S_{xy}=S_{yx}=\mu(y)\psi_{yy}+Bn \tag{23}$$

$$S_{xx}=0, S_{yy}=0, \tag{24}$$

And the dimensionless boundary conditions are

$$\left.\begin{array}{c} u\mp\gamma S_{xy}=0 \\ \theta\mp\beta_1\frac{\partial\theta}{\partial y}=0 \\ \left(E_1\frac{\partial^3}{\partial x^3}+E_2\frac{\partial^3}{\partial x\partial t^2}+E_3\frac{\partial^2}{\partial t\partial x}\right)y=\frac{\partial S_{xy}}{\partial y}-\frac{H^2\psi_y}{1+m^2}+\frac{Re}{(Fr)^2}sin\alpha \end{array}\right] \text{At } y=h_1,h_2, \tag{25}$$

Where

$$h_1=-1-m_1x-d_1\,(Cos(x-t)+\emptyset)\,,\ h_2=1+m_1x+d_2(Cos\,2\pi(x-t))$$

Furthermore, heat transfer coefficient at lower wall is derived as

$$Z=\frac{\partial h_1}{\partial x}\,\theta_y(h_1) \tag{26}$$

Through Eqs. (20) and (21), we obtain

$$\frac{\partial^2 S_{xy}}{\partial y^2}-\left(\frac{BrH^2}{(1+m^2)}+\frac{1}{\kappa}\right)\psi_{yy}=0 \tag{27}$$

We toke the dimensionless approximate expression for $\mu(y)$as

$\mu(y)=e^{-\epsilon y}=1-\epsilon y,$ where$\epsilon<1,$

ϵ is non- dimensional viscosity parameter.

3. Solution Methodology

By using the perturbation method for a small non- dimensional viscosity parameter ϵ and expanding the flow quantities in a power series of ϵ , we obtain

$$\psi=\psi_0+\epsilon\,\psi_1 \tag{28}$$

$$\theta = \theta_0 + \epsilon\, \theta_1 \tag{29}$$

Substituting Eqs. (28), (29) into Eqs. (22) - (27) and then comparing the coefficients of same power of ϵ up to the first order, we obtain the following two systems

3.1. Zeroth order system

The general form of zeroth- order system is: -

$$\psi_{0yyyy} - \left(\frac{H^2}{1+m^2} + \frac{1}{\kappa}\right)\psi_{0yy} = 0 \tag{30}$$

$$\theta_{0yy} + Br\left(\frac{\partial^2 \psi_0}{\partial y^2} + Bn\right)\psi_{0yy} + \frac{H^2}{1+m^2} Br {\psi_{0y}}^2 = 0 \tag{31}$$

Now with the respect to the boundary conditions, we have: -

$$\psi_{0y} \mp \gamma\left(\psi_{0yy} + Bn\right) = 0 \tag{32}$$

$$\theta_0 \mp \beta_1 \theta_0 y = 0 \tag{33}$$

$$E_1 \frac{\partial^3 y}{\partial x^3} + E_2 \frac{\partial^2 y}{\partial x \partial t^2} + E_3 \frac{\partial^2 y}{\partial t \partial x} = \psi_{0yyy} - \frac{H^2}{1+m^2}\psi_{0y} + \frac{Re}{(Fr)^2} sin\alpha \tag{34}$$

$at\ y = h_1, h_2,$

3.2. First order system

The general form of first- order system is

$$\psi_{1yyyy} - y\psi_{0yyyy} - 2\psi_{0yyy} - \left(\frac{H^2}{1+m^2} + \frac{1}{\kappa}\right)\psi_{1yy} = 0 \tag{35}$$

$$\frac{\partial^2 \theta}{\partial y^2} + Br\left(\psi_{1yy} - \psi_{0yy}\right)\psi_{1yy} + \frac{H^2}{1+m^2} Br {\psi_{1y}}^2 = 0 \tag{36}$$

With the respect to the boundary conditions

$$\psi_{1y} \mp \gamma\left(\psi_{1yy} - y\psi_{0yy}\right) = 0 \tag{37}$$

$$\theta_1 \mp \beta 1 \theta_{1y} = 0 \tag{38}$$

$$\psi_{1yyy} - \frac{H^2}{1+m^2}\psi_{1y} = 0 \tag{39}$$

Solving the both system using Mathematica program, we get the closed form for ψ, and θ

$$\psi = \frac{1}{{k_1}^2}(c_1 e^{k_1 y} + c_2 e^{-k_1 y}) + c_3 + y c_4 + \frac{\epsilon}{8{k_1}^3}(A_1 + A_2 + 8k_1(A_3 + {k_1}^2(c_7 + y c_8)),$$

$$\theta = -\frac{Br}{{k_1}^2 \kappa}(A_4 + A_5 + A_6) + n_1 + y n_2 - \frac{\epsilon}{3840 k1^6 \kappa} Br e^{-2k_1 y}(A_7 + A_8 + A_9 + A_{10} - A_{11}) + n_3 + y n_4,$$

Where

$A_1 = c_1 e^{k_1 y}(-3 - 2k_1 y + 2{k_1}^2 y^2)$,

$A_2 = c_2 e^{-k_1 y}\left(3 - 2k_1 y - 2{k_1}^2 y^2\right)$,

$A_3 = c_5 e^{k_1 y} + c_6 e^{-k_1 y}$,

$k_1 = \left(\frac{H^2}{1+m^2} + \frac{1}{\kappa}\right)^{1/2}$,

$A_4 = \left(c_1 c_2 y^2 - \frac{1}{2}c_4^2 {k_1}^2 y^2 + \frac{1}{2}c_4^2 {k_1}^4 y^2 \kappa\right)$,

$A_5 = \frac{c_2^2 e^{-2k_1 y}(-1+2{k_1}^2\kappa)}{4{k_1}^2} + \frac{c_1^2 e^{2k_1 y}(-1+2{k_1}^2\kappa)}{4{k_1}^2}$,

$A_6 = \frac{c_2 e^{-k_1 y}(2c_4 + Bnk_1\kappa - 2c_4{k_1}^2\kappa)}{k_1} + \frac{c_1 e^{k_1 y}(-2c_4 + Bnk_1\kappa + 2c_4{k_1}^2\kappa)}{k_1}$,

$A_7 = (15c_2^2(-27 + 16{k_1}^5 y^3\kappa + 8{k_1}^6 y^4\kappa + 2{k_1}^2(2y^2 + 9\kappa) - 8{k_1}^3(y^3 + 3y\kappa) - 4{k_1}^4(y^4 + 4y^2\kappa))$,

$A_8 = 5(3{c_1}^2 e^{4k_1 y}(-27 - 16{k_1}^5 y^3\kappa + 8{k_1}^6 y^4\kappa + 2{k_1}^2(2y^2 + 9\kappa) + 8{k_1}^3(y^3 + 3y\kappa) - 4{k_1}^4(y^4 + 4y^2\kappa))$,

$A_9 = 192{k_1}^2({c_6}^2(-1 + 2{k_1}^2\kappa) + 4c_6 e^{k_1 y}k_1(c_5 e^{k_1 y}k_1 y^2 + c_8(2 - 2{k_1}^2\kappa)) + e^{2k_1 y}(8c_5 c_8 e^{k_1 y}k_1(-1 + {k_1}^2\kappa) + 2{c_8}^2{k_1}^4 y^2(-1 + {k_1}^2\kappa) + {c_5}^2 e^{2k_1 y}(-1 + 2{k_1}^2\kappa)))$,

$A_{10} = 32c_1 e^{2k_1 y}k_1(3c_5 e^{2k_1 y}(2 + k_1 y - 2k1^3 y\kappa + 2{k_1}^4 y^2\kappa - {k_1}^2(y^2 + 3\kappa)) + k_1(6c_8 e^{k_1 y}(3 - 6k_1 y + 2{k_1}^2 y^2)(-1 + {k_1}^2\kappa) + c_6 k_1 y^2(-15 + 2k_1 y + {k_1}^2(y^2 + 6\kappa)))))$,

$A_{11} = 4c_2 k_1(120c_6(2 - k_1 y + 2{k_1}^3 y\kappa + 2{k_1}^4 y^2\kappa - {k_1}^2(y^2 + 3\kappa)) + e^{k_1 y}k_1(-240c_8(3 + 6k_1 y + 2{k_1}^2 y^2)(-1 + {k_1}^2\kappa) + e^{k_1 y}y^2(40c_5 k_1(-15 - 2k1y + {k_1}^2(y^2 + 6\kappa)) + c_1(375 - 60{k_1}^2(y^2 + 4\kappa) + 4{k_1}^4(y^4 + 15y^2\kappa)))$,

Where $c_1, c_2, c_3, c_4, c_5, c_6, c_7, c_8, n_1, n_2, n_3, n_4$,can be found using simple calculations.

4. Result and Discussions

In this section we visualize graphically the influence of different inclusive parameters on velocity profile, temperature distribution, heat transfer coefficient and trapping phenomenon.

4.1. Velocity Profile

Figures 1-3 elucidate the behavior of velocity profile against the following various important parameters $(E_1, E_2, E_3\ \kappa, m, H, \phi)$ and for fixed values of $(\epsilon = 0.04, \mathrm{Fr} = 0.8, \mathrm{Re} = 0.2, \alpha = \frac{\mathrm{Pi}}{2}, \gamma = 0.7, t = 0.1, \mathrm{d}_1 = 0.4, \mathrm{d}_2 = 0.4, x = 0.4, m_1 = 0.1)$. Fig.1 (a) is plotted to describe the effect of wall elasticity parameters on velocity profile. One can conclude a significant increase upon enhancement of wall rigidity and tension parameters respectively E_1, E_2 whereas the velocity profile slightly rises as mass characterization parameter E_3 increase. Similar observation is seen for enhanced values of permeability parameter κ and Hall number m on velocity curve i.e. $u(y)$ is increasing and these results are shown in **Figure 1(b)** and **Figure 2 (a).** A reversed situation for the larger magnitude of both Hartman number

H and Bingham number Bn are shown in **Figure 2 (b)** and **Figure 3 (a).** From **Figure 3 (b)**, we notice that the velocity profile enhances for higher values of phase difference parameter ϕ.

1. (b)

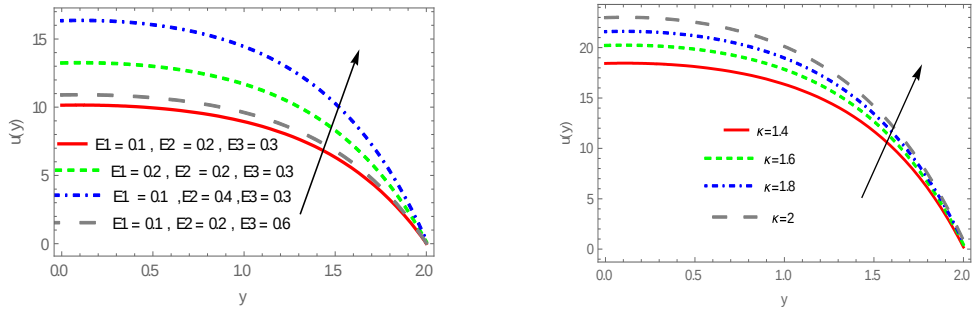

Figure 1:Velocity profile for different values of (a) Elasticity parameters E_1, E_2, E_3 (b) permeability parameter κ.

(a) (b)

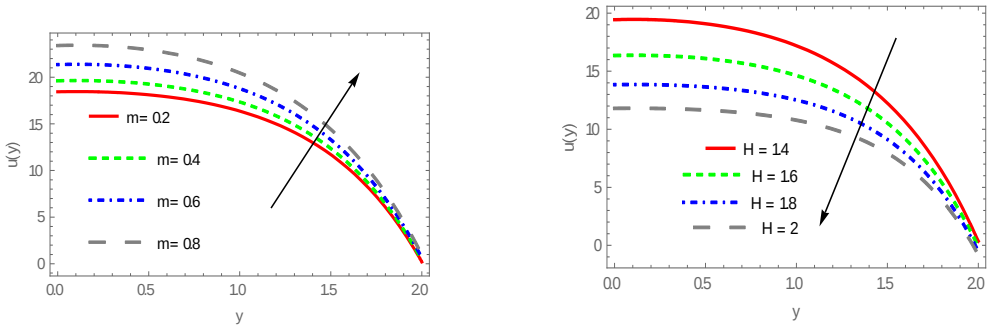

Figure 2: Velocity profile for different values of (a) Hall number m (b) Hartman number H ,

(a) (b)

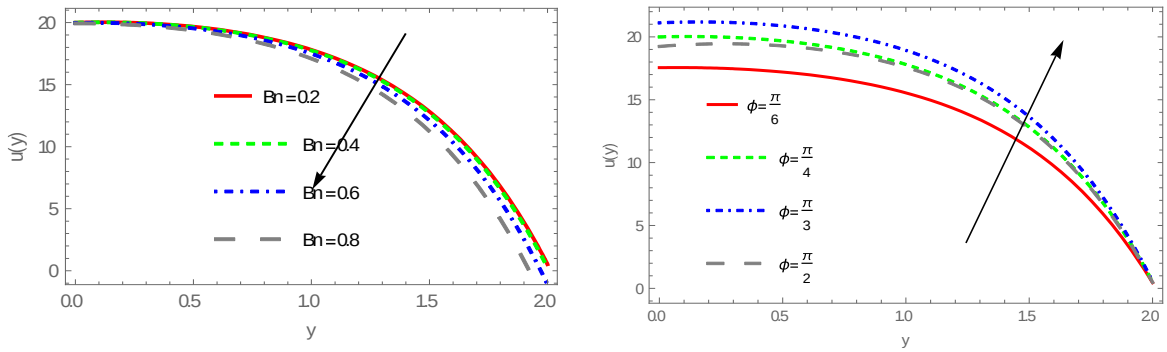

Figure 3: Velocity profile for different values of (a) Bingham number Bn (b) Phase difference parameter ϕ.

4.2. Temperature Distribution

Figures 4-6 are plotted to elaborate parabolic behavior for temperature distribution against axial y axis for different magnitudes of the parameters $(Br, Fr, H, \beta_1, m, Bn)$. **Figure** 4(a) illustrates the impact of Brinkman number on $\theta(y)$. It is seen that Br react directly on temperature profile. However, in **Figure 4(b)** Froude number Fr record quite opposite behavior compared to Brinkman number. The effect of Hartman number on temperature profile testified in Fig. 5(a). It is evident that the rise in Lorentz force produces a resistance for a larger value of Hartman number and consequently reduces the temperature profile. **Figures. 5(b), 6(a), and 6(b)** clarify an increment in temperature slip parameter β_1 Hall number m and Bingham number Bn causing rise in the temperature distribution curve.

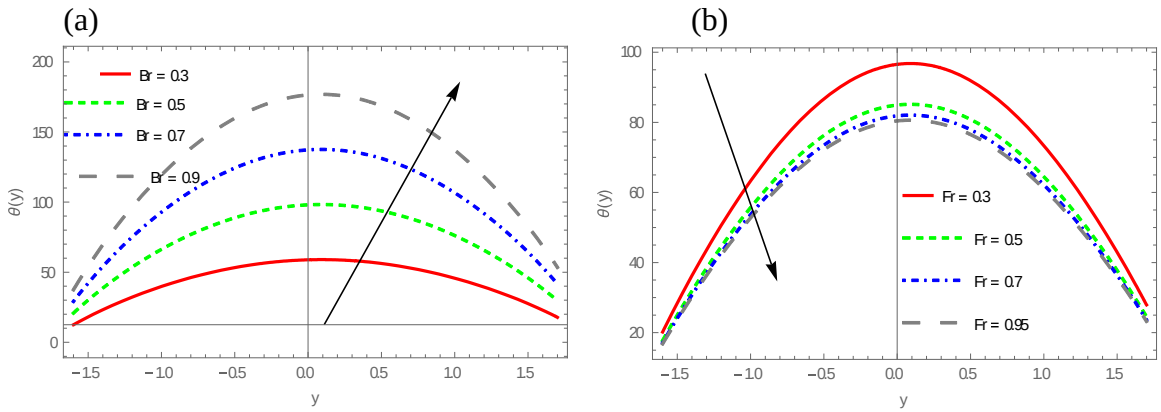

Figure 4: Temperature profile $\theta(y)$for different values of (a) Brinkman number Br (b) Froude number Fr.

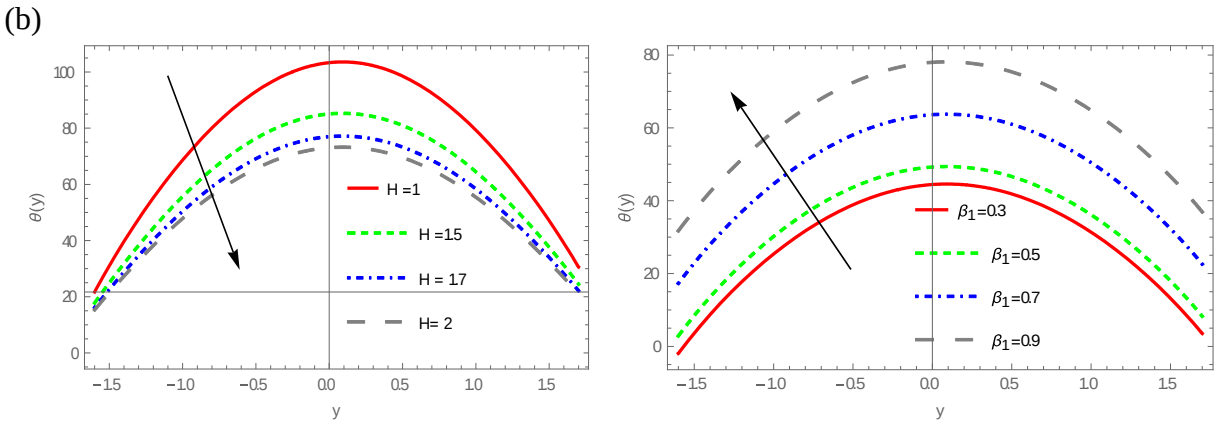

Figure 5: Temperature profile $\theta(y)$for different values of (a) Hartman number H (b) temperature slip parameter β_1.

(a) (b)

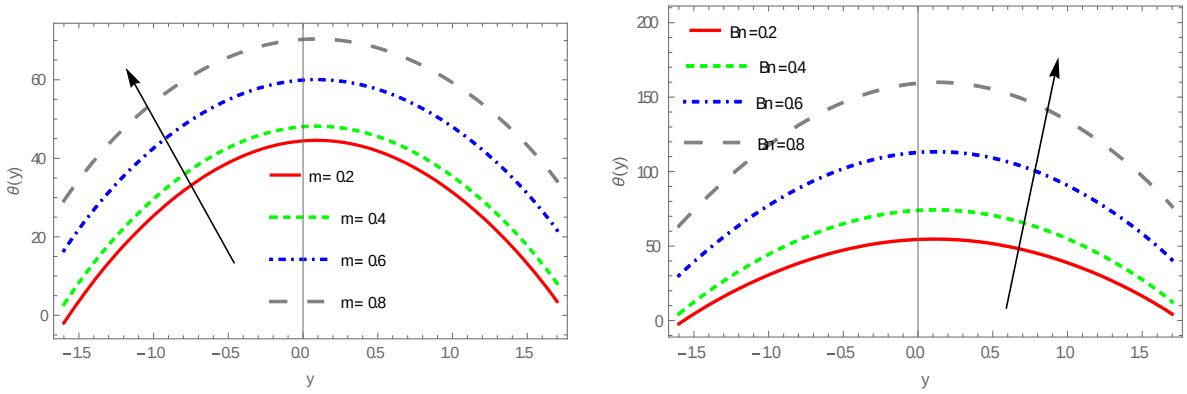

Figure 6: Temperature profile $\theta(y)$for different values of (a) Hall number m (b) Bingham number Bn.

4.3. Heat Transfer

Figures 7-8 elucide the impact of Brinkman number Br, Froude number Fr, phase difference parameter $\emptyset$, and permability parameter κ on the coefficient of heat transfer at the lower wall profile. These figures show an oscillatory behavior of $Z(x)$ via the flow of peristaltic waves along the channel wall. **Figure 7(a)** portrays the increasing function of heat transfer coffecient due to arise in Br value. However **Figure 7(b)** depicts an oppsite reaction for Fr. **Figure 8(a)** charactrizes a mixed behavior for $Z(x)$ for a higher value of $\emptyset$. We deduce from **Figure 8(b)** that for ascending magnitude of κ, the rate of heat transfer increases .

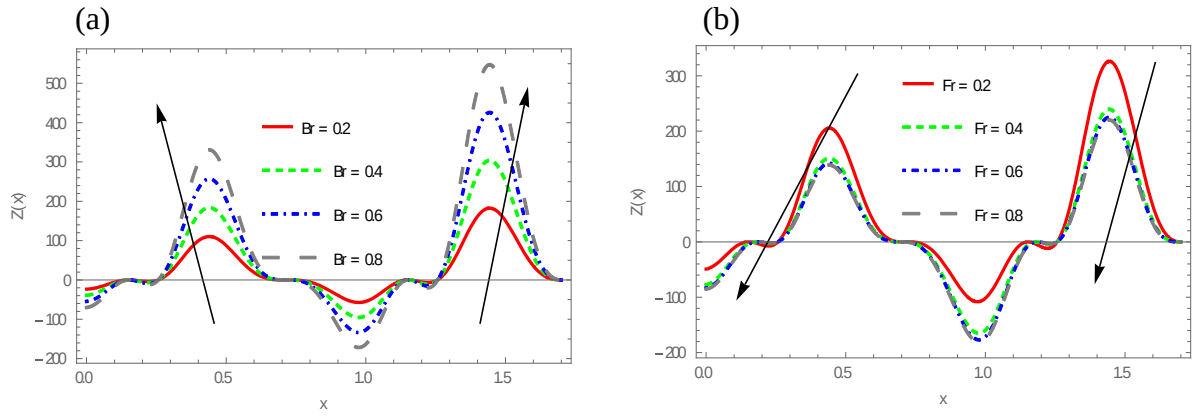

Figure 7: Heat transfer coefficient Z$(x)$for different values of (a) Brinkman number Br (b) Froude number Fr.

(a) (b)

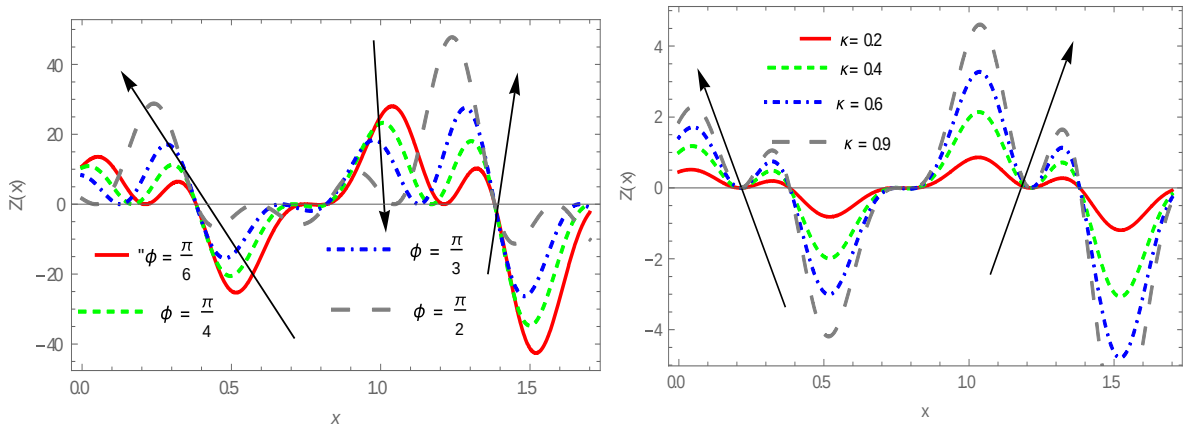

Figure 8: Heat transfer coefficient $Z(x)$ for different values of (a) Phase difference parameter ϕ (b) permeability parameter κ.

4.4. Trapping phenomenon

A phenomenon in which an amount of fluid trapped in closed streamlines is called bolus. In this part of work, some results of the phenomenon of trapping are portrayed. **Figures 9-15** highlight the impact of wall elasticity parameters E_1, E_2, E_3 and for $H, \kappa, m, \epsilon, Fr, Bn$ values. Graphical results show two asymmetric regions, the first region begins from $(0.2 \leq x \leq 0.7)$ while the second region $(0.7 \leq x \leq 1.2)$. One can observe an increment in size and number of trapped bolus, whereas the second region witnesses a less number of generated bolus. The effect of wall rigidity and tension parameters respectively E_1, E_2 and mass characterization parameter E_3 on trapping phenomenon are shown in **Figure 9**. However, it is important to note that both parameters E_1, E_2 increase the trap bolus in magnitude and number while a higher value of E_3 parameter that reduces the size of bolus but in the right side, its number reduces. **Figure 10** reveals that ascending value of Hartman number H is due to increases in Lorentz force which resists the fluid flow as a result decreases the size of trapping bolus. Opposite to this result, permeability parameter κ directly acts on trapping bolus in size and number; see **Figure 11**. The variation of Hall number m and dimensionless viscosity parameter ϵ on trapped bolus are reflected in **Figures 12** and **13**. One can observe the increasing function for them on trapped bolus size. In **Figure 14**, we demonstrate that a larger value of Froude number Fr reduces both the size and circulation of bolus. **Figure 15** interprets the independence of trapping bolus of variation of Bingham parameter Bn.

(a)

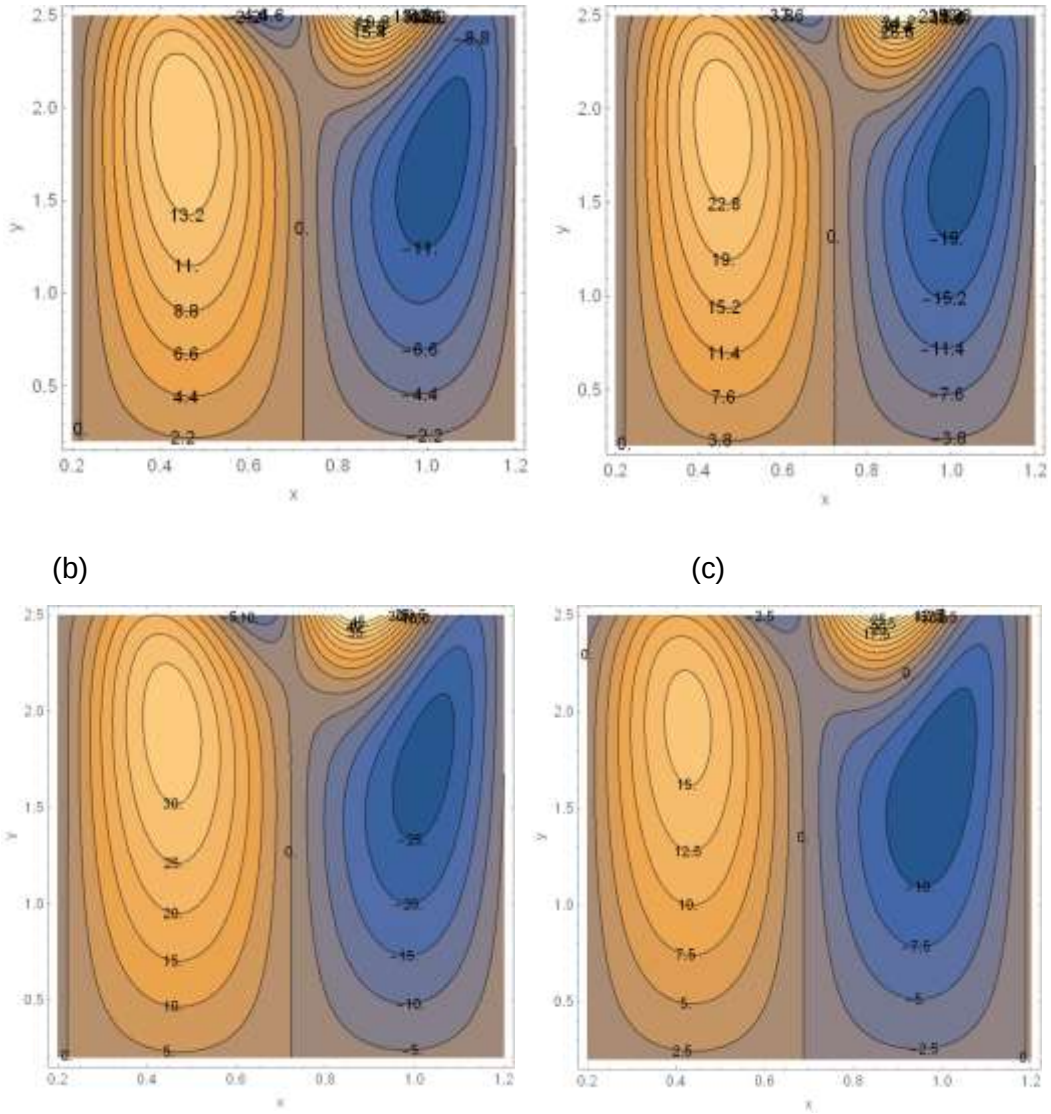

Figure 9: Streamlines for variation of parameters (a) wall rigidity E_1 (b) wall tension E_2 (c) mass characterization E_3 with $\epsilon = 0.02, \kappa = 0.2, m = 0.2, Fr = 0.8, H = 1, Re = 0.2, \alpha = \frac{Pi}{6}, \gamma = 0.7, \phi = \frac{Pi}{4}, t = 0.1, m_1 = 0.5, Bn = 0.5$.

(a) (b)

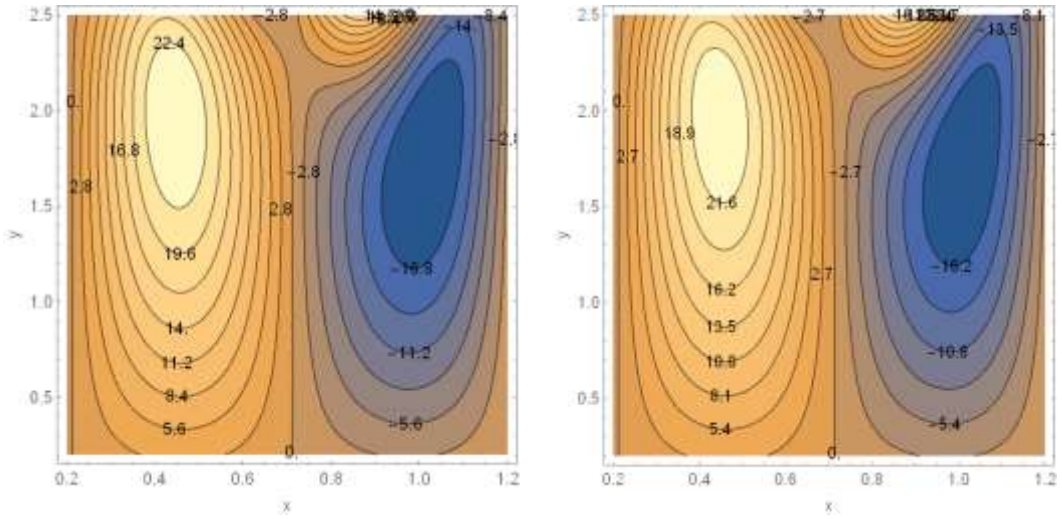

Figure 10 Streamlines for variation of Hartman number H with $E_1 = 0.4, E_2 = 0.2, E_3 = 0.3\ \epsilon = 0.02, \kappa = 0.2, m = 0.2, Fr = 0.8, d_1 = 0.1, Re = 0.2, \alpha = \frac{Pi}{6}, \gamma = 0.7, \phi = \frac{Pi}{4}, t = 0.1, m_1 = 0.5, Bn = 0.5$.

(a) (b)

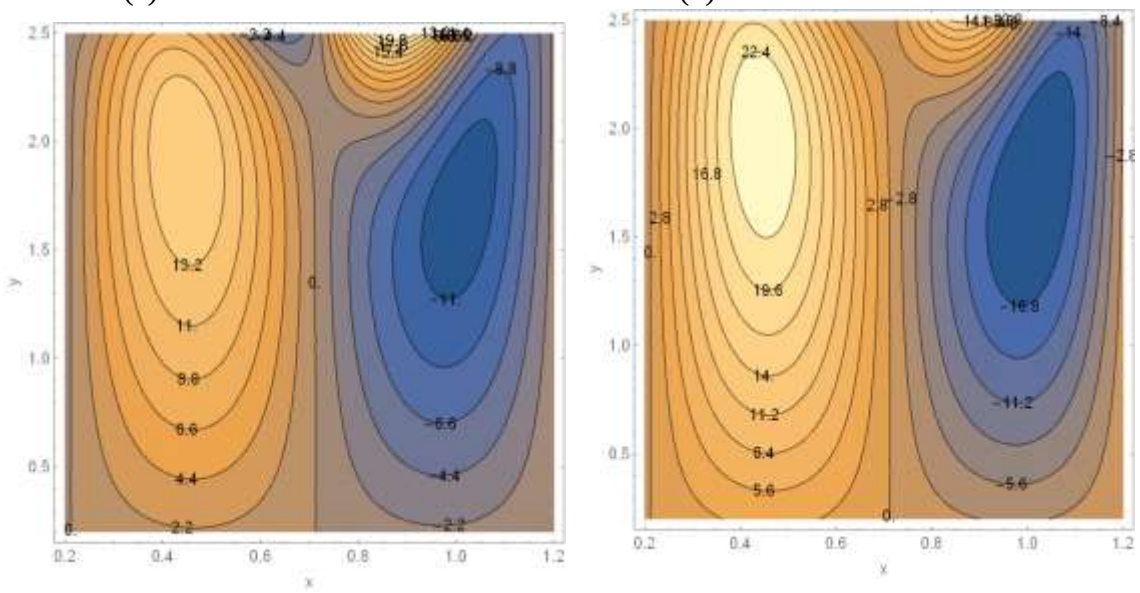

Figure 11 Streamlines for variation of permeability parameter κ with $E_1 = 0.4, E_2 = 0.2, E_3 = 0.3\ \epsilon = 0.02, H = 0.2, m = 0.2, Fr = 0.8, d_1 = 0.1, Re = 0.2, \alpha = \frac{Pi}{6}, \gamma = 0.7, \phi = \frac{Pi}{4}, t = 0.1, m_1 = 0.5, Bn = 0.5$.

(a) (b)

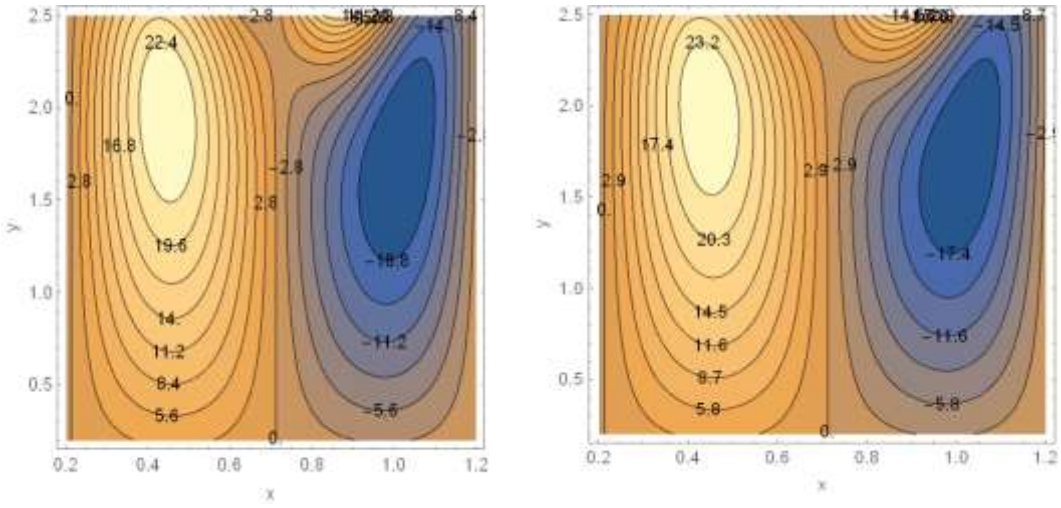

Figure 12 Streamlines for variation of Hall number m with $E_1 = 0.4, E_2 = 0.2, E_3 = 0.3\ \epsilon = 0.02, H = 0.2, \kappa = 0.2, Fr = 0.8, d_1 = 0.1, Re = 0.2, \alpha = \frac{Pi}{6}, \gamma = 0.7, \phi = \frac{Pi}{4}, t = 0.1, m_1 = 0.5, Bn = 0.5$.

(a) (b)

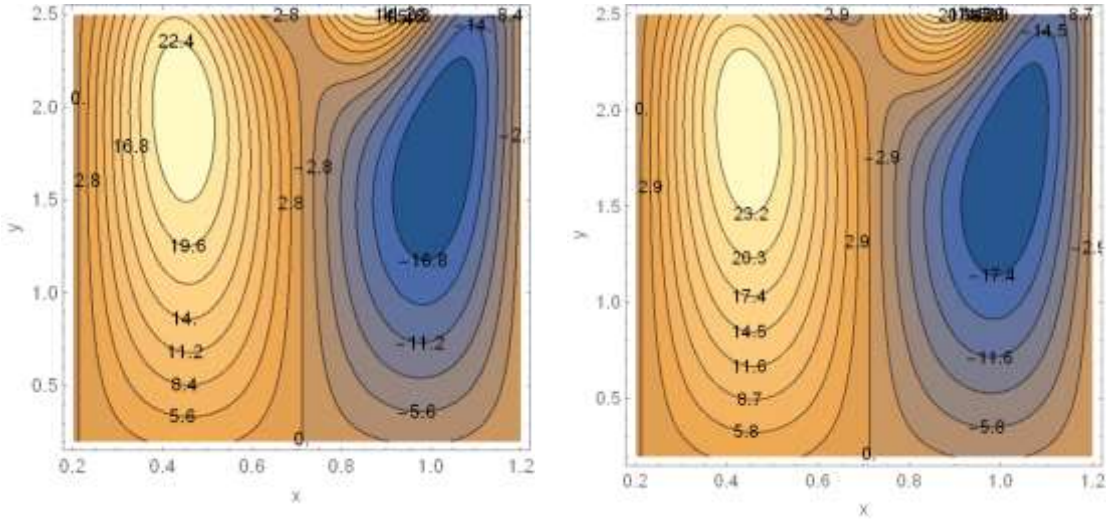

Figure 13 Streamlines for variation of non- dimensional viscosity parameter ϵ with $E_1 = 0.4, E_2 = 0.2, E_3 = 0.3\ m = 0.2, H = 0.2, \kappa = 0.2, Fr = 0.8, d_1 = 0.1, Re = 0.2, \alpha = \frac{Pi}{6}, \gamma = 0.7, \phi = \frac{Pi}{4}, t = 0.1, m_1 = 0.5, Bn = 0.5$.

(a) (b)

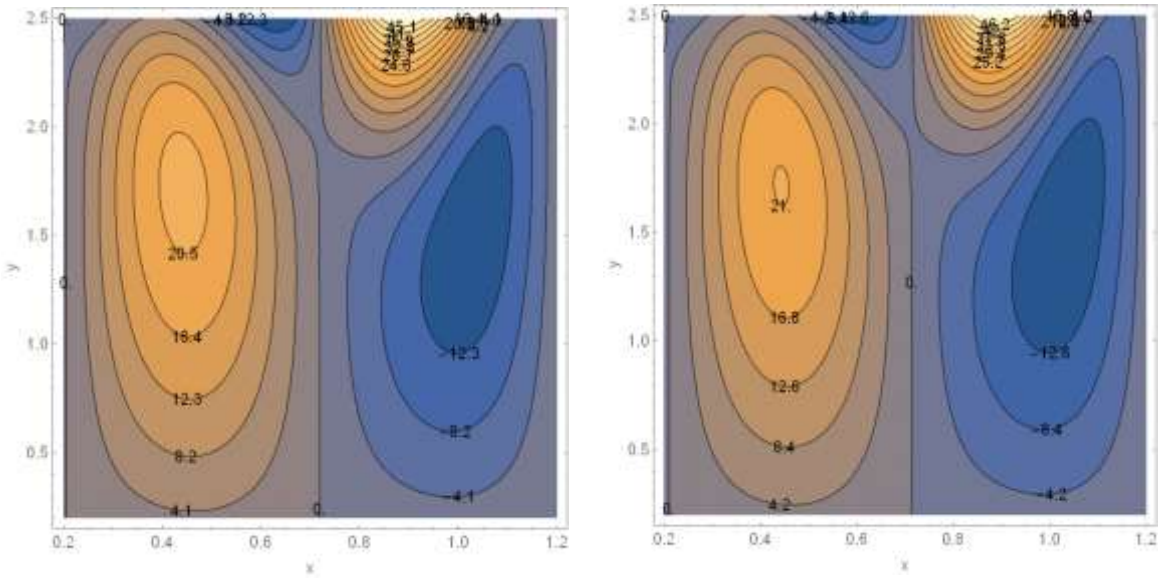

Figure 14 Streamlines for variation of Froude number Fr with $E_1 = 0.4, E_2 = 0.2, E_3 = 0.3\ m = 0.2, H = 0.2, \kappa = 0.2, \epsilon = 0.8, d_1 = 0.1, Re = 0.2, \alpha = \frac{Pi}{6}, \gamma = 0.7, \phi = \frac{Pi}{4}, t = 0.1, m_1 = 0.5, Bn = 0.5$.

(a) (b)

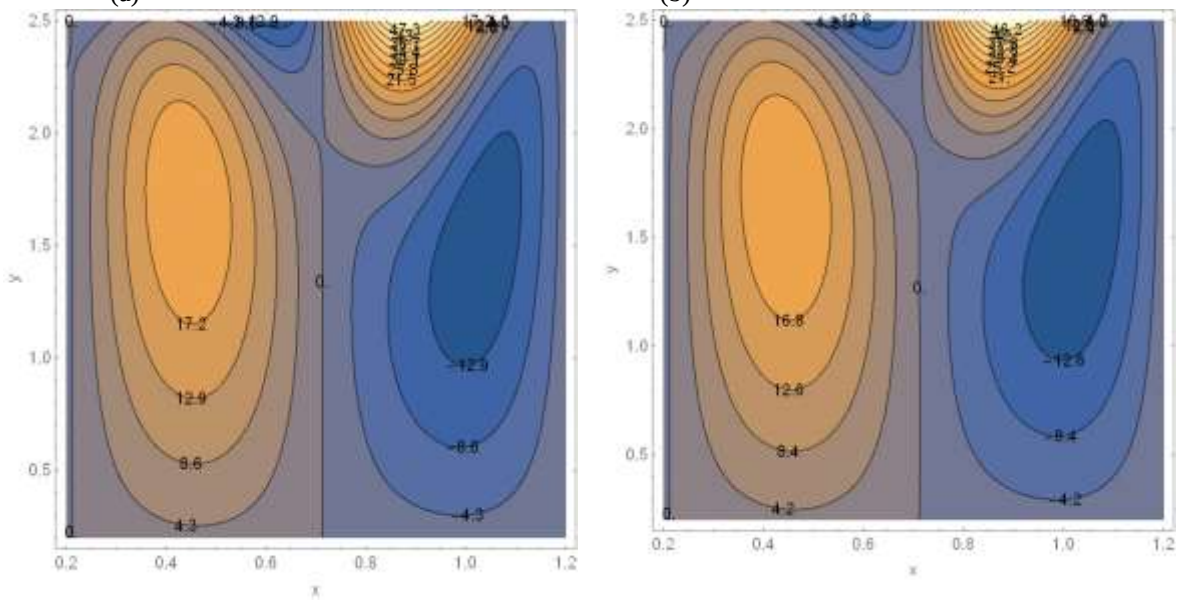

Figure 15 Streamlines for variation of Bingham number Bn with $E_1 = 0.4, E_2 = 0.2, E_3 = 0.3\ m = 0.2, H = 0.2, \kappa = 0.2, \epsilon = 0.8, d_1 = 0.1, Re = 0.2, \alpha = \frac{Pi}{6}, \gamma = 0.7, \phi = \frac{Pi}{4}, t = 0.1, m_1 = 0.5, Fr = 0.5$.

5. Conclusions

The peristaltic transport of non- Newtonian Bingham plastic fluid with variable viscosity in an inclined tapered asymmetric channel is performed, taking into account Hall and Joule's heating influences. Adopting assumptions of long wavelength and low Reynolds number the problem is modeled and reduced into a pair of nonlinear differential equations which are solved approximately by using a perturbation method. A parametric analysis is permitted through various graphs that made us outcome with some following important observations

1. The velocity profile is an increasing function of $m, \emptyset, \kappa$, and wall elasticity parameters whereas it decreases with arise up of H,and Bn parameters.

2. It is observed from the figures that the Froude number is oppositely affected by the temperature distribution profile.

3. Hartman number$H$ impact on temperature profile totally revers Hall number m effect i.e. the first one shows a reduction behavior while Hall number enhances it.

4. The absolute heat transfer shows an oscillatory behavior along the length of peristaltic wave as well as it depicts a mixed behavior for a larger value of phase difference parameter ϕ.

5. The trapping phenomenon is divided into two asymmetric regions, and from the figures one can notice that the trapped bolus increases in size and circulation as E_1, E_2 increase whereas it decreases for a higher magnitude of E_3.

6. The trapped bolus remains unchanged in size when Bingham number Bn enhances.

References

1. Mirsa,J.C.; Mallick, B.; Sinha, A. heat and mass transfer in asymmetric channel during peristaltic transport on MHD fluid having temperature-dependent properties, *Alexandria Eng*. **2018**,*57*, 391-406.

2. Hayat,T.; Igbal Rija; Tanveer Anum; Alsaedi,A. Influence of convective conditions in radiative peristaltic flow of pseudo plastic nano fluid in a tapered asymmetric channel, *J. Magn. Magn. Mater*. **2016**,408.

3. Adnan, F.A.; Abdualhadi, A.M. Effect of a magnetic field on a peristaltic transport of Bingham plastic fluid in asymmetrical channel. *Sci. int. (Lhore).***2019**, *31, 1*, 29-40.

4. Ali Nasir; Asghar Zaheer. Mixed convective heat transfer analysis for the peristaltic transport of visco plastic fluid: perturbation and numerical study, *Aip Advances***.2019,** *9*, 095001-1-9, 095001-10.

5. Hina, S.; Mustafa, M.; Hayat, T.; Alsaedi, A. Peristaltic flow of Powell-Eyring fluid in curved channel with heat transfer: A useful application in biomedicine, *Computer methods and programming in Biomedicine 135.* **2016,** 89-100.

6. Hayat, A.Ali; Ahmed, M. Abdulhadi. Analysis of Heat Transfer on Peristaltic Transport of Powell- Eyring Fluid in an Inclined Tapered Symmetric Channel with Hall and Ohm's Heating Influences, *Journal of AL-Qadisiyah for computer science and mathematics*.**2018,***10 ,2*.

7. Farah Alaa Adnan; Ahmad, M. Abdul Hadi. Effect of an inclined magnetic field on peristaltic flow of Bingham plastic fluid in an inclined symmetric channel with slip conditions, *Iraqi J. of Science*. **2019**, *60,7*, 1551-1574.

8. Farah Alaa Adnan; Ahmad, M. Abdul Hadi, peristaltic flow of the Bingham plastic fluid in a curved channel, *Ibn Al-Haitham J. pure & Appl. Sci.* **2019**, *32 ,3*.

9. Hayat, T; Farooq, S.; Mustafa, M.; Ahmed, B.; Ahmed, B. peristaltic transport of Bingham plastic fluid considering magnetic field, Soret and Dufour effects, *Results in physics*. **2017**, *7*, 2000-2011.

10. Lakshminarayana, P.; Sreenadh, S.; Sucharitha, G. The influence of slip, wall properties on the peristaltic transport of conducting Bingham fluid with heat transfer, *Procedia Eng*. **2015**, 127 1087-1094.

11. Ara, A.; Khan, N.A.; Sultan, F.; Ullah, S. Numerical Simulation of Jeffery- Hamel flow of Bingham Plastic fluid and Heat Transfer in the Presence of Magnetic Field, *Appl. Compute. Math*. **2019,** *18,2*, 135-148.

12. Dheia Gaze Salih, Influences of varying temperature and concentration on (MHD) peristaltic transport of Jeffery fluid with variable viscosity through porous channel, *DOI: 10.29304/jqcm.***2019***,11,3*,586.

13. Ahmad, T.S.; Abdulhadi, A.M. peristaltic transport of MHD flow and heat transfer in a tapered asymmetric channel through porous medium: effect of variable viscosity, velocity-non slip and temperature jump, *Int. j. of advance sci. tech. research*.**2017**, *7, 2*, 53-69.